Keep or discard

NRL Report 6698

Subcritical Flaw Growth in 9Ni-4Co-0.25C Steel - A Fatigue and Fractographic Investigation and Its Relationship to Plane Strain Fracture Toughness

T. W. Crooker, L. A. Cooley, E. A. Lange, and C. N. Freed

Strength of Metals Branch
Metallurgy Division

May 1, 1968

NAVAL RESEARCH LABORATORY
Washington, D.C.

CONTENTS

ABSTRACT

Fatigue crack propagation and plane strain fracture toughness (K_{Ic}) studies were conducted on a 9Ni-4Co-0.25C steel which had been quenched and tempered to a yield strength of 180 ksi. Fatigue specimens were cycled to failure in a room air environment under several combinations of cyclic and tensile mean loads. It was observed that fatigue crack propagation became unstable at a critical level of stress-intensity which led to rapid failure. This critical stress-intensity level in fatigue was consistently below the stress-intensity value for crack instability predicted by conventional rising load K_{Ic} tests.

Electron fractography studies were conducted on the fatigue surfaces. A gradual change in fracture surface appearance with cyclic stress-intensity level was found to occur. Fatigue striations predominated at low cyclic stress-intensity levels, changing to dimpled rupture at high cyclic stress-intensity levels. No abrupt change in fracture surface appearance was observed to coincide with the critical stress-intensity level in fatigue.

It is concluded from this study that, although K_{Ic} provides a lower-bound estimate of stress-intensity for terminal fracture in monotonic loading, subcritical flaw growth by fatigue in some high-strength materials may define a more conservative estimate of structural material performance.

PROBLEM STATUS

This report completes one phase of the problem. Work on other aspects of the problem is continuing.

AUTHORIZATION

NRL Problems M01-18 and F01-17
Projects RR 007-46-5420 and S-4607-11894

Manuscript submitted January 22, 1968.

SUBCRITICAL FLAW GROWTH IN 9Ni-4Co-0.25C STEEL — A FATIGUE AND FRACTOGRAPHIC INVESTIGATION AND ITS RELATIONSHIP TO PLANE STRAIN FRACTURE TOUGHNESS

INTRODUCTION

Subcritical flaw growth by fatigue is a potential failure mechanism for high-strength structural metals. It is important to develop a quantitative understanding of this failure mechanism in order to define the properties of structural materials and, further, to predict the fatigue life of structures.

The usefulness of employing the fracture mechanics stress-intensity factor (K) in analyzing the growth rate of fatigue cracks in high-strength structural metals is well documented (1-4). This procedure offers the opportunity to correlate subcritical flaw growth characteristics directly with the fracture mechanics failure parameter, plane strain fracture toughness (K_{Ic}).

This report discusses the fatigue crack propagation characteristics of a 9Ni-4Co-0.25C steel in terms of the cyclic stress-intensity factor range (ΔK). These characteristics are compared with the results of K_{Ic} tests on the same material. In addition, the fatigue surfaces were studied by electron fractography to ascertain the various microfracture mechanisms by which subcritical flaw growth occurs in this material.

MATERIAL

The material under investigation is a 9Ni-4Co-0.25C high-alloy commercial-production steel, quenched and tempered to a yield strength of 180 ksi. This steel was processed by a special melting practice involving vacuum-carbon-deoxidation of an electric furnace air-melt heat, followed by a vacuum-consumable-electrode-remelt. Test specimens were machined from 1-in.-thick plate stock which had been evenly crossrolled to minimize mechanical anisotropy.

The chemical composition of this steel is given in Table 1, and the mechanical properties are given in Table 2.

Table 1
Chemical Composition

Element	C	Mn	Si	P	S	Ni	Cr	Mo	Co	V
Wt - %	0.25	0.28	0.01	0.006	0.008	8.31	0.40	0.48	3.78	0.11

The material under investigation was studied in the as-received condition which consisted of the following mill heat treatment:

1. Normalize at 1600°F for 1 hour.
2. Austenitize at 1500°F for 1 hour, followed by an oil quench.
3. Temper at 1000°F with air cooling.

Table 2
Mechanical Properties

Specimen Orientation	Tension Test Data for 0.505-In.-Diam Specimen				Charpy-V Energy at 30°F (ft-lb)	1-in. Dynamic Tear Test Energy (ft-lb)
	0.2% YS (ksi)	UTS (ksi)	Elong. in 2-in. (%)	Reduction of Area (%)		
RW	183.2	195.0	17.0	61.0	40	1996
WR	—	—	—	—	38	—

*The orientations RW (perpendicular to the final rolling path) and WR (parallel to the final rolling path) are defined in "The Slow Growth and Rapid Propagation of Cracks. Second Report of a Special ASTM Committee," Mater. Res. Std. 1 (No. 5):389-393(1961)

Figure 1 shows the microstructure in a plane parallel to the crack propagation direction. The predominating structure appears to be that of tempered martensite (5). The material is banded (Fig. 1, top). It is not known if the banding results from a chemical segregation effect or the carbide dispersion. The grain size of this material is No. 8 and finer, and the R_c hardness in the plane of the fracture path is 42.

FATIGUE CRACK PROPAGATION

Experimental Procedure

Fatigue crack propagation tests were performed using single-edge-notched (SEN) specimens cycled in cantilever bending. A detail drawing of the fatigue specimen is shown in Fig. 2. The test section has nominal dimensions of 2.5-in. wide and 0.5-in. thick. The net thickness is reduced to 0.45-in. by side-grooving, which acts to suppress shear lip formation and promote a straight crack front. The edge-notch is nominally 0.5-in. deep, and fatigue crack propagation is allowed to extend the flaw to a maximum total depth of 1.5-in. Measurements of fatigue crack length are performed by a slide-mounted optical micrometer focused on the root surface of the side-groove. Special consideration is given to preparation of the side-groove surface in order to aid optical observations of the fatigue crack tip. Tool marks are polished from the surface, and a very light sandblast is applied. Sandblasting causes light reflected off the surface to be diffused, thus eliminating glare and causing the fatigue crack to appear in darker contrast with its surroundings. The combination of test-section thickness and side-groove geometry employed on this specimen results in a crack front of nearly uniform depth through the thickness, i.e., a straight crack front, thereby allowing accurate measurements from surface observations.

The fatigue crack propagation tests were run under constant load at 5 cpm. As the crack propagates through the test section, stress-intensity levels increase, thus producing a range of crack growth rates for study. The stress-intensity characteristics of the fatigue specimen are illustrated in Fig. 3, which is a plot of the stress-intensity factor (K) versus flaw size (a) for several values of constant load. Flaw size is defined as total crack depth measured from the specimen edge and includes the nominal 0.5-in. notch. These stress-intensity curves are computed from the equation derived by Kies (6). Nearly identical results can be obtained from Paris and Sih's equation (7), with a small correction made for side-grooves (8).

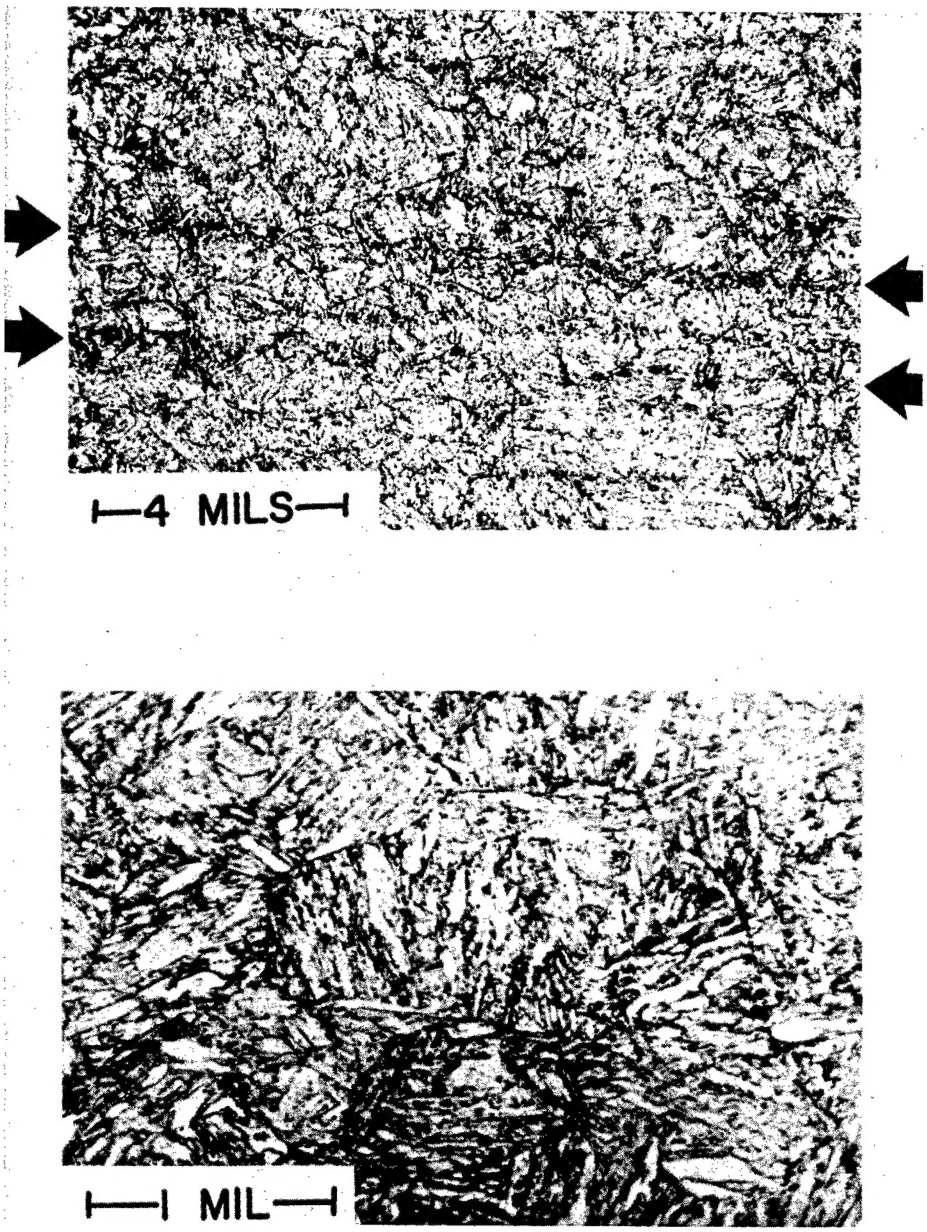

Fig. 1 - Microstructure in a plane parallel to the fracture path. A banded structure exists between arrows (top). Acidic acid plus nitric acid etch. Original magnification 500X (top), 2000X (bottom).

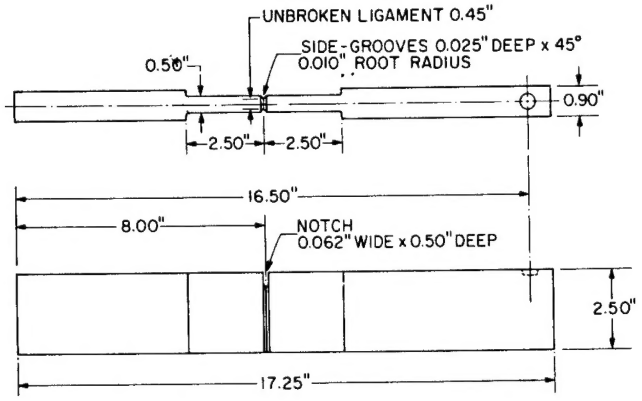

Fig. 2 - Details of the NRL single-edge-notched (SEN) cantilever fatigue specimen with side-grooves

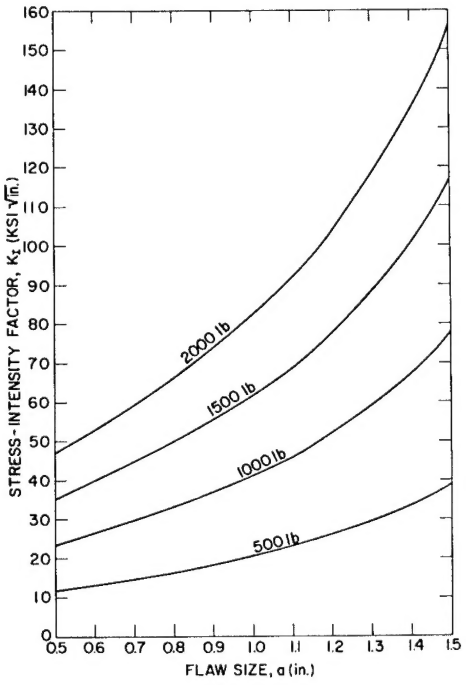

Fig. 3 - Stress-intensity characteristics of the SEN fatigue specimen as a function of flaw size for various constant loads. The curves were calculated from Kies' (6) equation.

A tensile cyclic load range of 1500 lb was used for all tests performed in this study. Using the term R to denote the load ratio (minimum load/maximum load), the following load ratios were used: R = -1.0 (-1500 to 1500 lb), R = 0 (0 to 1500 lb), R = 0.14 (250 to 1750 lb), and R = 0.25 (500 to 2000 lb).

Discussion of Results

The results of these tests are shown in Figs. 4 and 5, which are plots of flaw size versus cycles of repeated load. The slope of these curves is the fatigue crack growth rate. Load, flaw size, and specimen geometry define the stress-intensity factor. These parameters are displayed in Fig. 6, which is the conventional log-log plot of fatigue crack growth rate versus stress-intensity-factor range. Fatigue crack growth rates plotted as a function of stress-intensity-factor range provide a generalized means of displaying experimental results.

The results shown in Figs. 4 through 6 suggest the following observations on the growth of fatigue cracks. Although the tensile cyclic load range was held constant at 1500 lb, a significant reduction in the number of cycles required to cause specimen failure resulted from the application of tensile mean loads. Terminal fracture is determined by the maximum tensile load; therefore, the critical flaw size becomes smaller as mean loads are added. Additionally, the crack growth rates become greater as tensile mean load increases, even though the cyclic load remains constant. The crack growth rate data shown on Fig. 6 are grouped with the positive R values occupying the upper region of the scatter limits. These results strongly suggest that mean loads cannot safely be ignored in structural fatigue design situations where high strength materials are being employed.

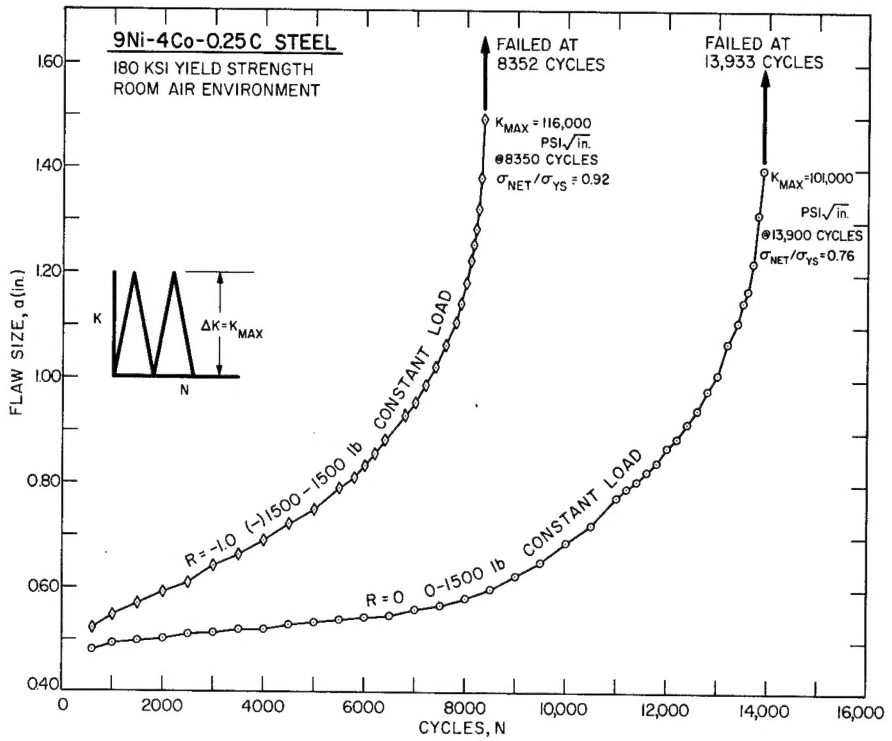

Fig. 4 - Fatigue crack propagation data for specimens cycled zero-to-tension (R = 0) and tension-to-compression (R = -1.0). The notations of K_{max} at the top of each curve refer to the last observation prior to terminal failure.

A second observation concerns the effect of compressive cyclic loading on fatigue crack growth. The specimen which was loaded tension-to-compression (R = -1.0) failed sooner than the specimen which was loaded zero-to-tension (R = 0), even though the maximum tensile load in each test was the same. This observation gains significance with the realization that the crack tip process zone in compression rapidly approached a region of low bending stresses as the crack front approached the centerline of the gross section, i.e., the fractured surfaces carried most of the compressive load. As a result, the compressive loading acted mainly to accelerate crack propagation in the early stages of the test. The growth rate data for this test shown on Fig. 6 were plotted using only the tensile stress-intensity-factor amplitude, and thereby ignoring the compressive half of the load. Using this analysis, there appears to be no difference between the growth rates for R = 0 and R = -1.0. This is not generally true, and, just as with tensile mean loads, compressive cyclic loading must be accounted for in sophisticated design procedures for fatigue (9).

All of the fatigue test specimens failed by brittle fracture before gross yielding could occur. Further, all of the specimens propagated fatigue cracks in a rapid, unstable manner at maximum stress-intensity levels well below K_{Ic}. The paramater K_{Ic} is the critical stress-intensity for initial crack instability under rising load in plane strain, and is taken to be a lower-bound estimate for crack instability. The K_{Ic} tests performed on this material are described in the Appendix. The value of K_{Ic} was established to be slightly in excess of 150,000 psi $\sqrt{in}$. Rapid fatigue crack propagation, leading to terminal failure in just a few cycles, began in all specimens at a maximum stress-intensity level very close to 100,000 psi $\sqrt{in}$. This was taken to be the critical

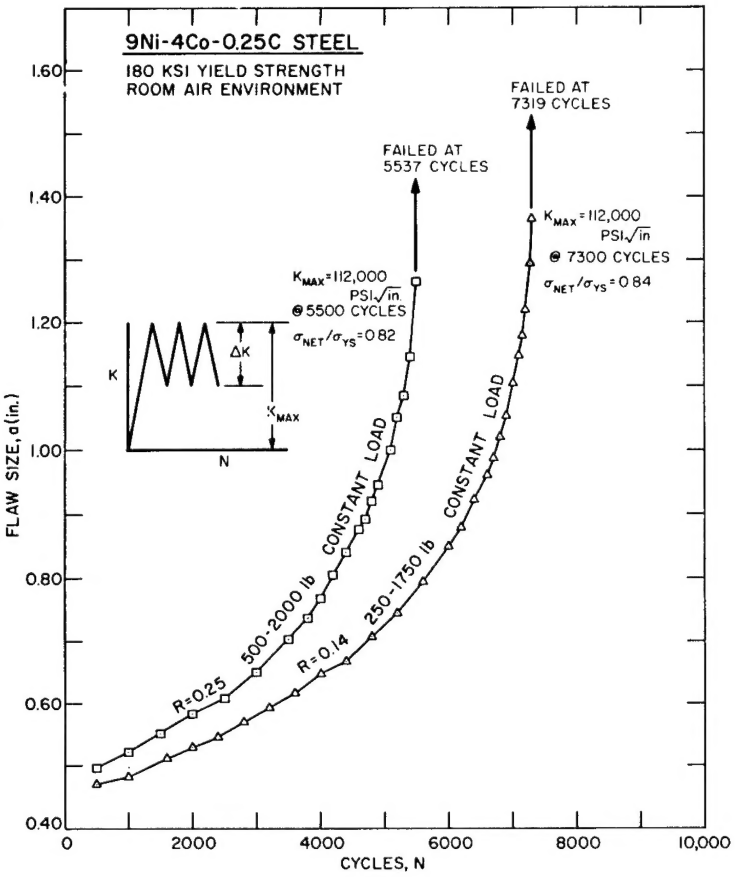

Fig. 5 - Fatigue crack propagation data for specimens cycled tension-to-tension (R = 0.14 and R = 0.25)

stress-intensity corresponding to the onset of rapid fatigue failure. However, based on macrosurface features, it appears that terminal fractures occurred at stress-intensity levels very close to K_{Ic}.

Unstable fatigue crack propagation in many high-strength materials has been observed by numerous researchers (2,4,9-11). However, the relationship of this phenomenon to K_{Ic} is not well established. This study and recent work by Clark and Wessel (11) suggest that unstable fatigue crack propagation can occur well below K_{Ic}. Unstable fatigue crack propagation may define an even more conservative limitation on the use of high strength materials than does plane strain fracture toughness.

Structural Performance Interpretation

The results of this study indicate that under cyclic loading the 9Ni-4Co-0.25C test material is limited to a maximum allowable stress-intensity level of approximately 100,000 psi $\sqrt{in}$. An interpretation of this service limitation is shown in Fig. 7, which is a plot of nominal stress level versus critical flaw depth for the specific stress-intensity level of 100,000 psi $\sqrt{in}$. Two curves are given on this plot; the upper curve is for a semicircular flaw (a/2c = 0.50), and the lower curve is for a long shallow flaw (a/2c = 0.10). The equation used to compute these curves applies to a surface flaw in a large plate loaded in tension (12).

The stress levels shown on Fig. 7 range from 50 to 100 percent of yield strength stress. Flaw sizes which would be sufficient to initiate rapid fatigue failure in this material are shown to range from <0.10 to 0.75 in. Thus, the service performance limitations of this high-strength steel become more apparent.

Structural fatigue life for this material can be computed by means of the fatigue crack growth rate relationship given in Fig. 6, starting with an assumed or measured initial flaw size as the lower limit and growing the crack by fatigue to a critical flaw size determined from Fig. 7.

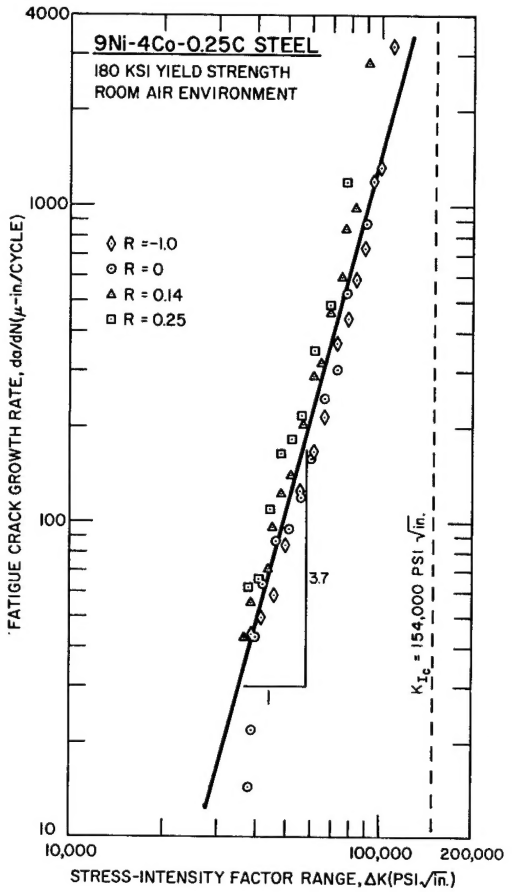

Fig. 6 - Log-log plot of fatigue crack growth rate as a function of stress-intensity-factor range

ELECTRON FRACTOGRAPHY

Experimental Procedure

Figure 8 shows the fracture surface developed for the fatigue specimen cycled in tension-to-tension bending with a load range of 250 to 1750 lb (R = 0.14). The portion of this surface examined with a two-stage cellulose-acetate replication technique lay within a medial strip approximately 13/64-in. wide extending from the notch root into the fast fracture region. Although not shown, identical areas from the "fixed" surface break of specimens cycled under loads of 0 to 1500 lb and 500 to 2000 lb were examined in the same fashion. The "fixed" surface belongs to that portion of the test specimen held by the supporting clamps and not subjected to movement by the loading jig.

Specimen surfaces were examined using the standard two-stage cellulose-acetate replication technique (13). Each replica was examined in a Siemans Elmiskop I electron microscope at a beam voltage of 40 kv. Magnifications ranged from 375X to 5000X with prints enlarged 3X. All areas photographed were taken as stereographic pairs, which facilitated interpretation of the various surface features.

Fracture Surface Topography

Replicas were taken from the "fixed" surfaces of three specimens. Fractographs shown are those from specimens cycled under loads of 250 to 1750 lb and 500 to 2000 lb. Tension-to-tension cycling minimizes surface rubbing, which is undesirable for fractographic studies. Although surface topography varied with individual replicas, the fractographs shown are typical for principal modes observed.

The first region studied encompasses the first 0.1 in. of crack growth, where a = 0.50 in. and $\Delta K = 36$ ksi $\sqrt{\text{in.}}$ Figures 9 and 10 are from the specimen loaded 250 to 1750 lb. The ruptured surface consists of broad, shallow striations (between the small arrows in

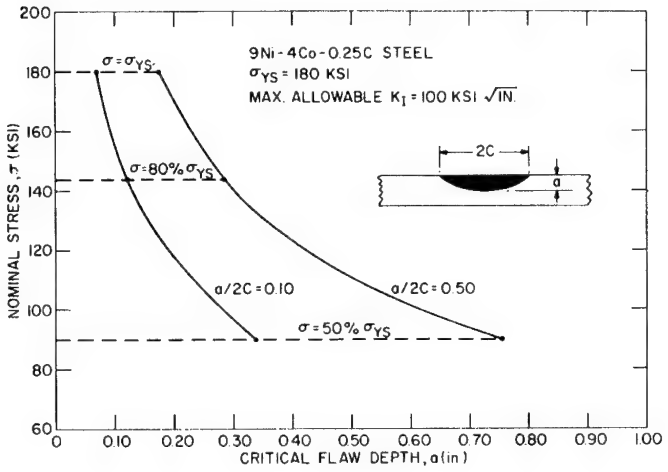

Fig. 7 - Relationships between nominal stress and critical flaw depth for 9Ni-4Co-0.25C steel at 180 ksi YS. The curves are computed from the equation for an embedded surface flaw in a large tension-loaded plate (12).

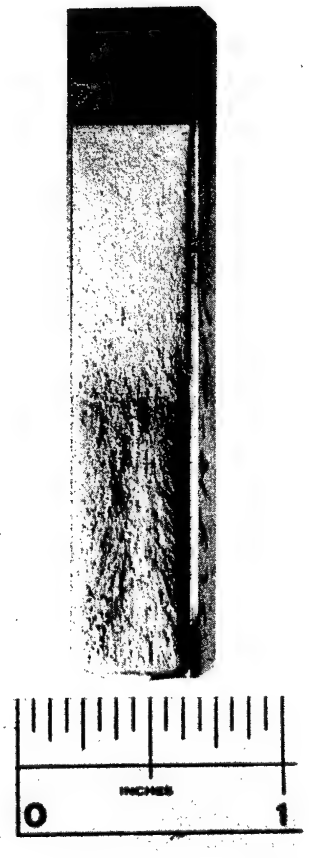

Fig. 8 - Fracture surface from the specimen cycled in tension-to-tension bending with load range of 250 to 1750 lb (R = 0.14)

Fig. 9) or tongues and ridges as seen in Fig. 10. The broad, shallow striations comprised 40 to 60 percent of the surface examined. At higher magnifications (Fig. 11) fatigue striations in the specimen loaded 500 to 2000 lb are broad and shallow with the edges of the individual striations outlined by discontinuous tongues. A further illustration of the surface complexity in this region is shown in Fig. 12. Shallow striations appear in the upper left, with shallow, equiaxed dimples in the lower left portions of the fractograph.

As the crack front advances to the second area studied, the broad, shallow striations disappear. For flaw sizes ranging from 0.7 to 0.9 in., the surface of the specimen loaded 250 to 1750 lb consists of shallow dimples and random tear ridges as in Fig. 13 or shallow, equiaxed dimples as in Fig. 14. These features comprised approximately 80 percent of the areas examined.

The third area studied is from the region where the fatigue crack was propagating rapidly. Figure 15 shows topography of this region for the specimen cycled in 500 to 2000 lb tension. At flaw sizes ranging from 1.0 to 1.20 in., shallow equiaxed dimples, in places nucleated by inclusions, are the prevalent mode.

The final area studied lies within the region of fast, terminal fracture. The separation consists exclusively of dimpled rupture. Figure 16 illustrates this feature obtained from the specimen loaded 500 to 2000 lb. The microfracture mode is dimpled rupture with no single dimple size predominating.

Fig. 9 - Tension-to-tension fatigue markings in a specimen loaded from 250 to 1750 lb. A packet of striations is shown between the large arrows while individual striations appear between the small arrows.

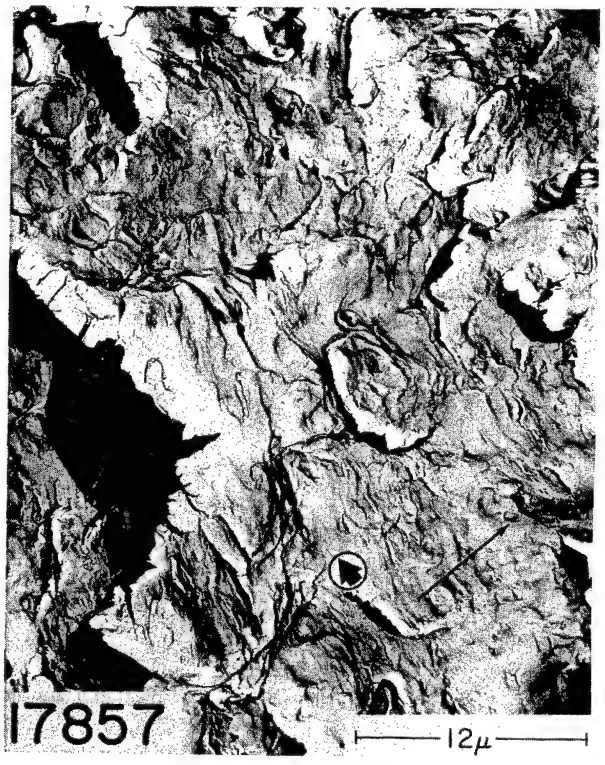

Fig. 10 - Tension-to-tension fatigue markings in a specimen loaded from 250 to 1750 lb. Numerous tongues and ridges aligned parallel with the large arrow are normal to crack propagation path indicated by the long arrow.

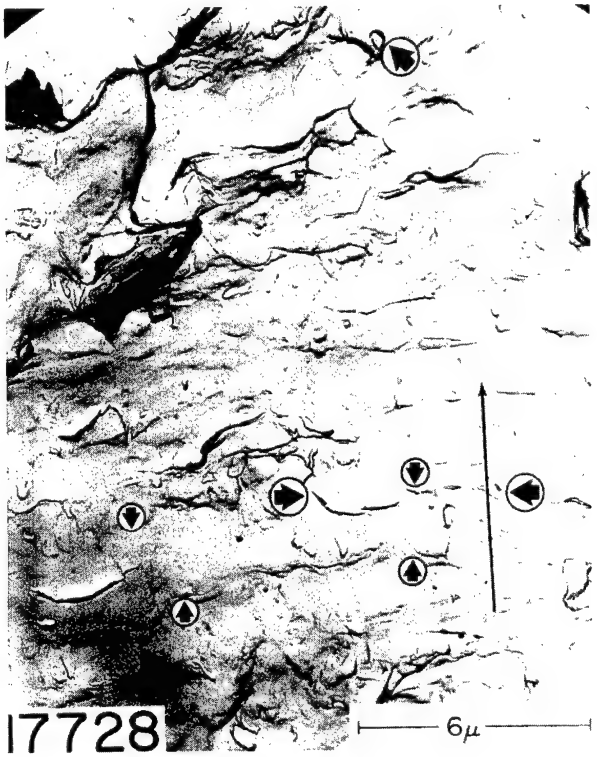

Fig. 11 - Tension-to-tension fatigue markings in a specimen loaded from 500 to 2000 lb. An individual striation is shown between the small arrows; a series of tongues and ridges delineating the separation of two striations is shown between the pair of large arrows.

Fig. 12 - Tension-to-tension fatigue markings in a specimen loaded from 250 to 1750 lb. The surface consists of broad, shallow striations (upper right), shallow equiaxed dimples (lower left), and ridges (left center).

Fig. 13 - Tension-to-tension fatigue markings in a specimen loaded from 250 to 1750 lb. The surface consists of shallow dimples and tear ridges orientated in a random fashion to the fracture path.

Fig. 14 - Tension-to-tension fatigue markings in a specimen loaded from 250 to 1750 lb. The surface consists of shallow dimples.

Fig. 15 - Region of fast fatigue for tension-to-tension bending in a specimen loaded from 500 to 2000 lb. The surface consists exclusively of shallow dimples. The arrows indicate dimple formation from inclusions.

Fig. 16 - Region of fast fracture for a specimen loaded from 500 to 2000 lb. The surface consists of large and small dimples.

Discussion of Results

Names of surface features, and their association with either ductile or brittle fracture modes, are those evolved and proposed at NRL by Beachem, Dahlberg, and coworkers (13-18).

Features common to all surfaces examined were dimples, tongues, ridges, and striations. Dimples are characteristic of ductile rupture modes involving plastic flow in the vicinity of the advancing crack tip (18). The nature of dimples shown in Figs. 12, 13, and 14 suggests normal dimpled rupture during successive stages of cyclic load growth before final coalescence and linkage with the advancing crack front.

Tongues and ridges are features generally associated with cleavage or quasi-cleavage, both of which are brittle failure modes. However, their association with generally undulating surfaces rather than plateau like areas is indicative of plastic tearing. Quasi-cleavage is indicative of environmental cracking, such as stress corrosion (19). The lack of positive evidence to indicate that quasi-cleavage was a prevalent separation mode is also indicative that environmental crack growth was not significant.

Striations, a feature common to fatigue crack propagation, may be of either a ductile or brittle mode, depending on the material and the hypothesized propagation model (20). In a study by Hertzberg (21), it was shown that striation formation was influenced by the orientation of certain slip planes and slip directions with the advancing crack. Other researchers have shown that striations are affected by a material's stacking fault energy (22). Materials having high stacking fault energies show ill-defined striations because of the ease of cross slip.

In this present study no attempt was made to ascertain the effects of grain orientations or stacking fault energies on the fracture process. Dimple formation was probably facilitated by inclusions and carbide particles. There is no conclusive evidence to support preferential grain boundary growth or a theory for dimple inoculation at grain boundaries.

Figure 17 summarizes the various aspects of crack propagation. During initial stages of crack growth with $\Delta K = 36$ ksi $\sqrt{\text{in.}}$ the morphology consists of broad striations or tear ridges parallel to the crack front. Crack extension results from local plastic separation at the crack tip during successive load cycles.

As the crack front progresses to the point indicated by $\Delta K = 47$ ksi $\sqrt{\text{in.}}$ evidences of fatigue striations vanish and predominating features are shallow dimples and tear ridges. Crack growth results from the interaction of plastic separation at the tip and dimple formation in discrete regions ahead of the tip.

In the region of fast fatigue, where $\Delta K = 73$ ksi $\sqrt{\text{in.}}$, the crack advances by coalescence of voids forming ahead of the tip. No outstanding change was detected between this region and that of fast fracture. Dimpled rupture was characteristic for both regions, and it was impossible to delineate the point of separation between the two by electron fractography.

SUMMARY AND CONCLUSIONS

Subcritical flaw growth was studied in samples of a commercial production 9Ni-4Co-0.25C steel, quench-and-temper heat treated to a yield strength of 180 ksi. The study consisted of a series of fatigue crack propagation tests, conducted in a room air environment, followed by an electron fractographic investigation of the fatigue surfaces. The fatigue data were analyzed using the fracture mechanics stress-intensity factor K. The

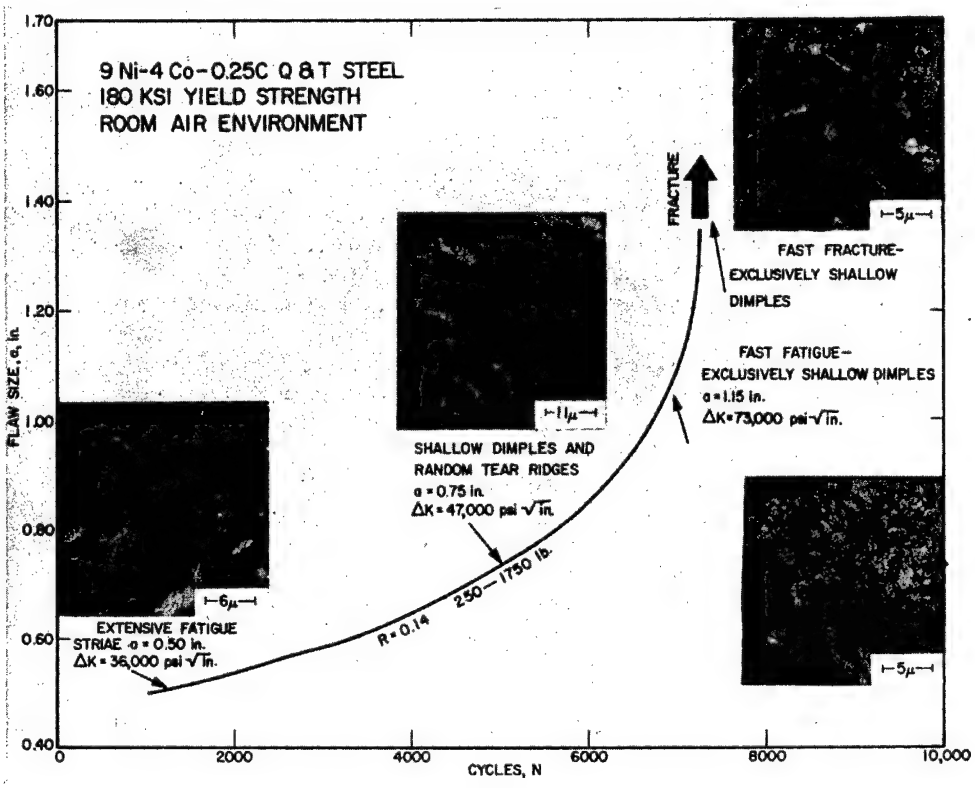

Fig. 17 - Variation of microfracture surface topography with increasing stress-intensity level. The surface changes gradually from one consisting of striations to one consisting of dimples. No change in microfracture mode was apparent in regions of fast fatigue and fast fracture.

fatigue performance of the test material was compared with plane strain fracture toughness (K_{Ic}) data.

The following conclusions have been reached from this investigation:

1. A satisfactory correlation was found to exist between the rate of fatigue crack growth, da/dN, and the cyclic tensile stress-intensity factor range, ΔK. This relationship is of the form $da/dN = c\ (\Delta K)^{3.7}$, which is in close agreement with Paris' fourth-power law for fatigue crack propagation. However, tensile mean loads and compressive cyclic loads were observed to exert a significant effect upon both crack growth rates and cycles to terminal failure.

2. Very rapid fatigue crack propagation was observed to occur at cyclic stress-intensity amplitudes well below K_{Ic}. This suggests a critical stress-intensity level for fatigue failure which is more conservative than the failure criterion for monotonic loading. However, terminal failure of the fatigue specimens corresponded very closely with predictions based on K_{Ic} measurements.

3. The fractographic examination illustrates the fact that high-stress fatigue failures cannot be classified as such solely on the presence or absence of striations, a fact of importance to the failure analyst.

4. A gradual change in fracture surface appearance with increasing cyclic stress-intensity level was found to occur. No abrupt change in fracture surface appearance was seen to coincide with the critical stress-intensity level in fatigue.

5. There was no positive evidence to support a hypothesis that environmental cracking was significant in the fracture process.

ACKNOWLEDGMENTS

The authors acknowledge the helpful efforts of the following individuals: Mrs. S. M. McCoy, who performed the metallography; Mr. R. J. Hicks, who conducted the fatigue tests; and Mr. D. H. Price, who performed the macrofractography. Dr. E. P. Dahlberg provided helpful criticism of the fractographic interpretation.

REFERENCES

1. Paris, P.C., "The Fracture Mechanics Approach to Fatigue," in "Fatigue-An Interdisciplinary Approach," Proceedings Tenth Sagamore Army Materials Research Conference, Aug. 13-16, 1963, New York:Syracuse University Press, pp. 107-127, 1964

2. Carman, C.M. and Katlin, J.M., "Low-Cycle Fatigue Crack Propagation Characteristics of High Strength Steels," J. Basic Eng., 88 (No. 4) (1966)

3. Brothers, A.J. and Yukawa, S., "Fatigue Crack Propagation in Low-Alloy Heat-Treated Steels," J. Basic Eng. 89 (No. 1) pp. 19-27 (1967)

4. Clark, W.G., Jr., "Subcritical Crack Growth and Its Effect Upon the Fatigue Characteristics of Structural Alloys," "National Symposium on Fracture Mechanics," Lehigh University, Bethlehem, Pennsylvania, June 19-21, 1967

5. Boniszewski, T., "Discussion 1 on the Martensite Transformation," in "Physical Properties of Martensite and Bainite," Iron Steel Inst. (London) Spec. Report 93, pp. 20-24, 1965

6. Kies, J.A., Smith, H.L., Romine, H.E., and Bernstein, H., "Fracture Testing of Weldments," in "Fracture Toughness Testing and Its Applications," Am. Soc. Testing Mater., Spec. Tech. Publ. 381, pp. 328-356 (1965)

7. Paris, P.C. and Sih, G.C., "Stress Analysis of Crack," in "Fracture Toughness Testing and Its Applications," Am. Soc. Testing Mater., Spec. Tech. Publ. 381, pp. 30-81 (1965)

8. Freed, C.N. and Krafft, J.M., "Effect of Side Grooving on Measurements of Plane-Strain Fracture Toughness," J. Mater. 1 (No. 4):770-790, Dec. 1966

9. Crooker, T.W. and Lange, E.A., "Low Cycle Fatigue Crack Propagation Resistance of Materials for Large Welded Structures," in "Fatigue Crack Propagation," Am. Soc. Testing Mater., Spec. Tech. Publ. 415, pp. 94-127 (1967)

10. Johnson, H.H. and Paris, P.C., "Sub-Critical Flaw Growth," Cornell University, Materials Science Center, Report No. 730, July 25, 1967 (submitted to the Journal of Engineering Fracture Mechanics)

11. Clark, W.G., Jr. and Wessel, E.T., "Interpretation of the Fracture Behavior of 5456-H321 Aluminum with WOL Toughness Specimens," Westinghouse Research Laboratories, Scientific Paper 67-1D6-BTLFR-P4, Sept. 8, 1967

12. Tiffany, C.F. and Masters, J.N., "Applied Fracture Mechanics," in "Fracture Toughness Testing and Its Applications," Am. Soc. Testing Mater., Spec. Tech. Publ. 381, pp. 249-277 (1965)

13. Beachem, C.D., "The Interpretation of Electron Microscope Fractographs," NRL Report 6360, Jan. 21, 1966

14. Beachem, C.D., "Electron Microscope Fracture Examination to Characterize and Identify Modes of Fracture," NRL Report 6293, Sept. 28, 1965

15. Beachem, C.D. and Meyn, D.A., "Illustrated Glossary of Fractographic Terms — Section 2," NRL Memorandum Report 1547, June 1964

16. Beachem, C.D., Brown, B.F., and Edwards, A.J., "Characterizing Fractures by Electron Fractography — Part 12: Quasi-Cleavage," NRL Memorandum Report 1432, June 1963

17. Dahlberg, E.P. and Beachem, C.D., "Fractography — Part 15. Some Artifacts Possible With the Two-Stage Plastic Carbon Replication Technique," NRL Memorandum Report 1457, Sept. 1963

18. Beachem, C.D. and Pelloux, R.M.N., "Electron Fractography — A Tool for the Study of Micromechanisms of Fracturing Processes," in "Fracture Toughness Testing and Its Applications, Am. Soc. Testing Mater., Spec. Tech. Publ. 381, pp. 210-245 (1965)

19. Judy, R.W., Jr., Crooker, T.W., Morey, R.E., Lange, E.A., and Goode, R.J., "Low-Cycle Fatigue-Crack Propagation and Fractographic Investigation of Ti-7A1-2Cb-1Ta and Ti-6A1-4V in Air and in Aqueous Environments," Am. Soc. Metals, Trans. Quart. 59 (No. 2):195-207, (1966)

20. Meyn, D.A., "Observations on Micromechanisms of Fatigue Crack Propagation in 2024 Aluminum," NRL Memorandum Report 1707, June 1966

21. Hertzberg, R.W., "Fatigue Fracture Surface Appearance," in "Fatigue Crack Propagation, Am. Soc. Testing Mater., Spec. Tech. Publ. 415, pp. 205-225 (1967)

22. Burghard, H.C., Jr. and Davidson, D.L., "Fracture Mechanisms and Fracture Surface Topography," Proceedings First International Conference on Fracture, Sendai, Japan, 1965, pp. 579-596

Appendix

FRACTURE TOUGHNESS TESTS

Fracture toughness tests were performed on the test material to determine the value of the plane strain fracture toughness parameter K_{Ic}, a material constant. K_{Ic} provides a lower-bound estimate of the stress-intensity that will cause unstable crack extension under a single application of rising load.

The K_{Ic} values presented in this report were obtained using single-edge-notched (SEN) tension specimens. The SEN specimen is modeled after the one employed by Miss A. M. Sullivan,* and her experimental compliance calibration was applied in the calculation of K_{Ic} values. The fracture specimens, shown in Fig. A1, are nominally 1 in. thick. The edge-notch is extended approximately 0.10 in. by a fatigue crack propagated at low stresses to assure maximum notch acuity.

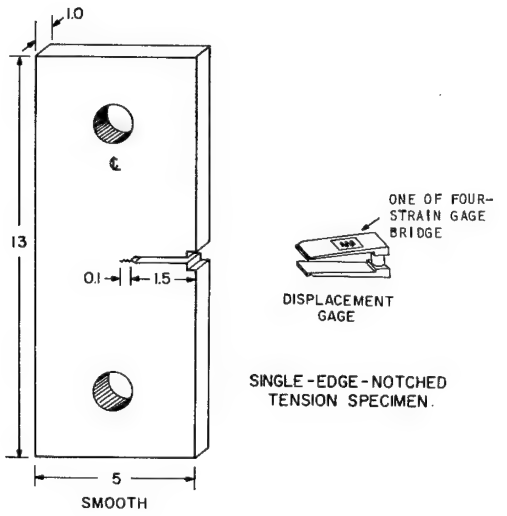

Fig. A1 - The SEN plane strain fracture toughness specimen and beam-type displacement gage employed in the K_{Ic} tests.

The load-displacement graph for each K_{Ic} test was drawn on an autographic X-Y recorder. These curves are shown in Fig. A2. Detection of initial crack extension was made by a beam-type displacement gage instrument with a strain gage circuit, also shown in Fig. A1.

The plane-strain fracture toughness data, obtained at room temperature, for the 9Ni-4Co-0.25C steel under investigation appears in Table A1. Specimens were tested in two fracture path orientations: perpendicular to the final rolling path (RW)† and parallel

*A.M. Sullivan, "New Specimen Design for Plane-Strain Fracture Toughness Tests," Mater. Res. Std. 4 (No. 1) (1964).

†"The Slow Growth and Rapid Propagation of Cracks," Second Report of a Special ASTM Committee, Materials Research and Standards, 1 (No. 5):389-393, (1961).

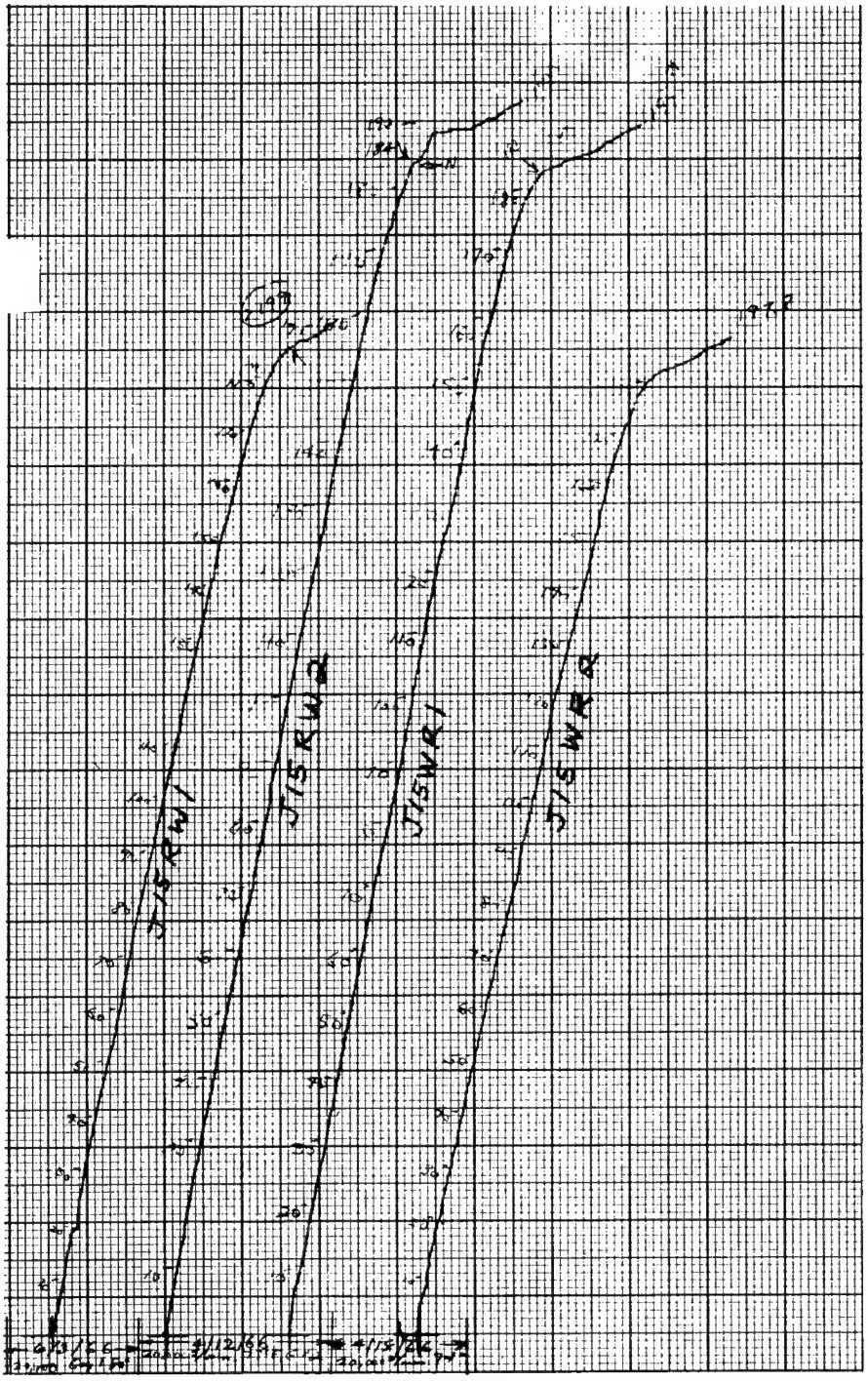

Fig. A2 - The autographic load-displacement graphs for each of the four K_{Ic} tests conducted on the 9Ni-4Co-0.25C test material

Table A1
Plane Strain Fracture Toughness Data

Fracture Direction	Number of Specimens	K Values (ksi $\sqrt{in}$)	Nominal Fracture Stress to Yield Stress Ratio, σ_n/σ_{YS}
RW	2	155-156	0.72
WR	2	152-155	0.72

to the final rolling path (WR).* The test material was evenly crossrolled and showed identical fracture toughness values in both orientations.

Among the criteria used to determine the validity of the K_{Ic} values was the requirement that the specimen thickness equal at least 2.5 times the plane-stress plastic zone size $2r_y$, where $2r_y = (1/\pi)(K/\sigma_{YS})^2$.† The K_{Ic} values reported in Table A1 include a plastic zone correction.

*"The Slow Growth and Rapid Propagation of Cracks," Second Report of a Special ASTM Committee, Materials Research and Standards, 1 (No. 5):389-393, (1961).
†Freed, C.N., "A Comparison of Fracture Toughness Parameters for Titanium Alloys," J. Eng. Fracture Mech. (publication pending).

Security Classification

DOCUMENT CONTROL DATA - R & D

(Security classification of title, body of abstract and indexing annotation must be entered when the overall report is classified)

1. ORIGINATING ACTIVITY (Corporate author)	2a. REPORT SECURITY CLASSIFICATION
Naval Research Laboratory Washington, D.C. 20390	Unclassified
	2b. GROUP

3. REPORT TITLE

SUBCRITICAL FLAW GROWTH IN 9Ni-4Co-0.25C STEEL — A FATIGUE AND FRACTOGRAPHIC INVESTIGATION AND ITS RELATIONSHIP TO PLANE STRAIN FRACTURE TOUGHNESS

4. DESCRIPTIVE NOTES (Type of report and inclusive dates) This report completes one phase of the problem. Work on other aspects of the problem is continuing.

5. AUTHOR(S) (First name, middle initial, last name)

T.W. Crooker, L.A. Cooley, E.A. Lange, and C.N. Freed

6. REPORT DATE	7a. TOTAL NO. OF PAGES	7b. NO. OF REFS
May 1, 1968	24	22

8a. CONTRACT OR GRANT NO.	9a. ORIGINATOR'S REPORT NUMBER(S)
NRL Problems M01-18 and F01-17 b. PROJECT NO. RR 007-01-46-5420 c. S-4607-11894 d.	NRL Report 6698 9b. OTHER REPORT NO(S) (Any other numbers that may be assigned this report)

10. DISTRIBUTION STATEMENT

This document has been approved for public release and sale; its distribution is unlimited.

11. SUPPLEMENTARY NOTES	12. SPONSORING MILITARY ACTIVITY
	Dept. of the Navy (Office of Naval Research and Naval Ship Systems Command) Washington, D.C. 20360

13. ABSTRACT

Fatigue crack propagation and plane strain fracture toughness (K_{Ic}) studies were conducted on a 9Ni-4Co-0.25C steel which had been quenched and tempered to a yield strength of 180 ksi. Fatigue specimens were cycled to failure in a room air environment under several combinations of cyclic and tensile mean loads. It was observed that fatigue crack propagation became unstable at a critical level of stress-intensity which led to rapid failure. This critical stress-intensity level in fatigue was consistently below the stress-intensity value for crack instability predicted by conventional rising load K_{Ic} tests.

Electron fractography studies were conducted on the fatigue surfaces. A gradual change in fracture surface appearance with cyclic stress-intensity level was found to occur. Fatigue striations predominated at low cyclic stress-intensity levels, changing to dimpled rupture at high cyclic stress-intensity levels. No abrupt change in fracture surface appearance was observed to coincide with the critical stress-intensity level in fatigue.

It is concluded from this study that, although K_{Ic} provides a lower-bound estimate of stress-intensity for terminal fracture in monotonic loading, subcritical flaw growth by fatigue in some high-strength materials may define a more conservative estimate of structural material performance.

DD FORM 1 NOV 65 1473 (PAGE 1)

S/N 0101-807-6801

Security Classification

UNCLASSIFIED

Naval Research Laboratory. Report 6698. SUBCRITICAL FLAW GROWTH IN 9Ni-4Co-0.25C STEEL — A FATIGUE AND FRACTOGRAPHIC INVESTIGATION AND ITS RELATIONSHIP TO PLANE STRAIN FRACTURE TOUGHNESS, by T.W. Crooker, L.A. Cooley, E.A. Lange, and C.N. Freed. 24 pp. and figs, May 1, 1968.

Fatigue crack propagation and plane strain fracture toughness (K_{Ic}) studies were conducted on a 9Ni-4Co-0.25C steel which had been quenched and tempered to a yield strength of 180 ksi. Fatigue specimens were cycled to failure in a room air environment under several combinations of cyclic and tensile mean loads. It was observed that fatigue crack propagation became unstable at a critical level of stress-intensity which led to rapid failure. This

UNCLASSIFIED (over)

1. Steel — Fatigue
2. Cracks — Propagation
3. Fractography
4. Fracture

I. Crooker, T.W.
II. Cooley, L.A.
III. Lange, E.A.
IV. Freed, C.N.

UNCLASSIFIED

Naval Research Laboratory. Report 6698. SUBCRITICAL FLAW GROWTH IN 9Ni-4Co-0.25C STEEL — A FATIGUE AND FRACTOGRAPHIC INVESTIGATION AND ITS RELATIONSHIP TO PLANE STRAIN FRACTURE TOUGHNESS, by T.W. Crooker, L.A. Cooley, E.A. Lange, and C.N. Freed. 24 pp. and figs, May 1, 1968.

Fatigue crack propagation and plane strain fracture toughness (K_{Ic}) studies were conducted on a 9Ni-4Co-0.25C steel which had been quenched and tempered to a yield strength of 180 ksi. Fatigue specimens were cycled to failure in a room air environment under several combinations of cyclic and tensile mean loads. It was observed that fatigue crack propagation became unstable at a critical level of stress-intensity which led to rapid failure. This

UNCLASSIFIED (over)

1. Steel — Fatigue
2. Cracks — Propagation
3. Fractography
4. Fracture

I. Crooker, T.W.
II. Cooley, L.A.
III. Lange, E.A.
IV. Freed, C.N.

UNCLASSIFIED

Naval Research Laboratory. Report 6698. SUBCRITICAL FLAW GROWTH IN 9Ni-4Co-0.25C STEEL — A FATIGUE AND FRACTOGRAPHIC INVESTIGATION AND ITS RELATIONSHIP TO PLANE STRAIN FRACTURE TOUGHNESS, by T.W. Crooker, L.A. Cooley, E.A. Lange, and C.N. Freed. 24 pp. and figs, May 1, 1968.

Fatigue crack propagation and plane strain fracture toughness (K_{Ic}) studies were conducted on a 9Ni-4Co-0.25C steel which had been quenched and tempered to a yield strength of 180 ksi. Fatigue specimens were cycled to failure in a room air environment under several combinations of cyclic and tensile mean loads. It was observed that fatigue crack propagation became unstable at a critical level of stress-intensity which led to rapid failure. This

UNCLASSIFIED (over)

1. Steel — Fatigue
2. Cracks — Propagation
3. Fractography
4. Fracture

I. Crooker, T.W.
II. Cooley, L.A.
III. Lange, E.A.
IV. Freed, C.N.

UNCLASSIFIED

Naval Research Laboratory. Report 6698. SUBCRITICAL FLAW GROWTH IN 9Ni-4Co-0.25C STEEL — A FATIGUE AND FRACTOGRAPHIC INVESTIGATION AND ITS RELATIONSHIP TO PLANE STRAIN FRACTURE TOUGHNESS, by T.W. Crooker, L.A. Cooley, E.A. Lange, and C.N. Freed. 24 pp. and figs, May 1, 1968.

Fatigue crack propagation and plane strain fracture toughness (K_{Ic}) studies were conducted on a 9Ni-4Co-0.25C steel which had been quenched and tempered to a yield strength of 180 ksi. Fatigue specimens were cycled to failure in a room air environment under several combinations of cyclic and tensile mean loads. It was observed that fatigue crack propagation became unstable at a critical level of stress-intensity which led to rapid failure. This

UNCLASSIFIED (over)

1. Steel — Fatigue
2. Cracks — Propagation
3. Fractography
4. Fracture

I. Crooker, T.W.
II. Cooley, L.A.
III. Lange, E.A.
IV. Freed, C.N.

UNCLASSIFIED

critical stress-intensity level in fatigue was consistently below the stress-intensity value for crack instability predicted by conventional rising load K_{Ic} tests.

Electron fractography studies were conducted on the fatigue surfaces. A gradual change in fracture surface appearance with cyclic stress-intensity level was found to occur. Fatigue striations predominated at low cyclic stress-intensity levels, changing to dimpled rupture at high cyclic stress-intensity levels. No abrupt change in fracture surface appearance was observed to coincide with the critical stress-intensity level in fatigue.

It is concluded from this study that, although K_{Ic} provides a lower-bound estimate of stress-intensity for terminal fracture in monotonic loading, subcritical flaw growth by fatigue in some high-strength materials may define a more conservative estimate of structural material performance.

UNCLASSIFIED

UNCLASSIFIED

critical stress-intensity level in fatigue was consistently below the stress-intensity value for crack instability predicted by conventional rising load K_{Ic} tests.

Electron fractography studies were conducted on the fatigue surfaces. A gradual change in fracture surface appearance with cyclic stress-intensity level was found to occur. Fatigue striations predominated at low cyclic stress-intensity levels, changing to dimpled rupture at high cyclic stress-intensity levels. No abrupt change in fracture surface appearance was observed to coincide with the critical stress-intensity level in fatigue.

It is concluded from this study that, although K_{Ic} provides a lower-bound estimate of stress-intensity for terminal fracture in monotonic loading, subcritical flaw growth by fatigue in some high-strength materials may define a more conservative estimate of structural material performance.

UNCLASSIFIED

UNCLASSIFIED

critical stress-intensity level in fatigue was consistently below the stress-intensity value for crack instability predicted by conventional rising load K_{Ic} tests.

Electron fractography studies were conducted on the fatigue surfaces. A gradual change in fracture surface appearance with cyclic stress-intensity level was found to occur. Fatigue striations predominated at low cyclic stress-intensity levels, changing to dimpled rupture at high cyclic stress-intensity levels. No abrupt change in fracture surface appearance was observed to coincide with the critical stress-intensity level in fatigue.

It is concluded from this study that, although K_{Ic} provides a lower-bound estimate of stress-intensity for terminal fracture in monotonic loading, subcritical flaw growth by fatigue in some high-strength materials may define a more conservative estimate of structural material performance.

UNCLASSIFIED

UNCLASSIFIED

critical stress-intensity level in fatigue was consistently below the stress-intensity value for crack instability predicted by conventional rising load K_{Ic} tests.

Electron fractography studies were conducted on the fatigue surfaces. A gradual change in fracture surface appearance with cyclic stress-intensity level was found to occur. Fatigue striations predominated at low cyclic stress-intensity levels, changing to dimpled rupture at high cyclic stress-intensity levels. No abrupt change in fracture surface appearance was observed to coincide with the critical stress-intensity level in fatigue.

It is concluded from this study that, although K_{Ic} provides a lower-bound estimate of stress-intensity for terminal fracture in monotonic loading, subcritical flaw growth by fatigue in some high-strength materials may define a more conservative estimate of structural material performance.

UNCLASSIFIED